République Algérienne Démocratique et Populaire

Ministère de l'Enseignement Supérieur et de la Recherche Scientifique

École Nationale Polytechnique

Département d'Électronique

Ecole Doctorale Génie Electrique

Mémoire de Magister

Option : ***Systèmes de télécommunication***

Thème

"Blind source separation in time frequency domain using contrast functions"

Présenté par : Abdelkrim BOUCHOUATA

Soutenue le 14 Juillet 2010, devant le jury composé de :

Mohamed TRABELSI	*Professeur (ENP)*	*Président*
Hicham BOUSBIA-SALAH	*Maître de Conférences Classe A (ENP)*	*Examinateurs*
Abderrahmane AMROUCHE	*Maître de Conférences Classe A (USTHB)*	
Adel BELOUCHRANI	*Professeur (ENP)*	*Encadreur*

Année universitaire 2009-2010

Ecole Nationale Polytechnique 10, Avenue Hassen Badi, El-Harrach, Alger

ملخص

هذه الأطروحة تقدم تطبيق تقنيات جديدة لفصل الأعمى للإشارات مستغلا التواقيع وقت - تردد. المنهج المقترح يعتمد على توزيعات وقت – تردد. وتعرض أيضا اثنان من دوال التباين القائمة على تلك التوزيعات في إطار إشارات غير ثابتة. تستعمل خوارزميات تكرارية ذات انحدار نسبي لتحسين الدوال المقترحة وذلك للتحصل على فصل الإشارات.

الكلمات الرئيسية : الفصل الأعمى للإشارات، توزيعات وقت – تردد ، إشارات غير ثابتة ، خوارزميات تكرارية ، دوال التباين .

RESUME

Cette thèse présente l'implémentation de nouvelles techniques de séparation aveugle de sources qui exploitent les signatures temps-fréquence des signaux source. L'approche proposée repose sur les distributions temps-fréquence (DTF). Deux fonctions de contraste à base de DTF sont présentées pour des sources non-stationnaires. Des algorithmes itératifs utilisant la technique du gradient relatif sont utilisés pour optimiser les fonctions proposées et effectuer la separararation de sources.

Mots clés : séparation aveugle de sources, distributions temps-fréquence, signaux non-stationnaires, algorithmes itératifs, fonctions de contraste.

ABSTRACT

This thesis presents the implementation of new blind source separation techniques exploiting the time-frequency signatures of the source signals. The proposed approach relies on time-frequency distributions (TFD). Two TFD-based contrast functions are presented for non-stationary sources. Iterative algorithms using the relative gradient technique are used to optimize the proposed functions and perform source separararation.

Keywords: blind source separation, time-frequency distributions, non-stationary signals, iterative algorithms, contrast functions.

ACKNOWLEDGMENTS

All praise is due to Allah. Furthermore I would like to thank my mentor, Professor Adel Belouchrani for his unfathomable patience and his wide knowledge that he was always able to share. For their record breaking response time, the members of the Jury, MM Trabelsi, Bousbia-Salah, and Amrouche deserve my eternal gratitude. And last but not least, thanks go to all the members of my first circle, my close family.

PREFACE

Blind source separation (BSS) is becoming on of the most promising techniques in many areas in signal processing: wireless communications, biomedical, and audio applications [9]. The problem under consideration consist of recovering the original waveforms of the user emitted signals without any prior knowledge on their linear mixture, which can be either instantaneous or convolutive. The problem of blindly separating sources has two inherently indeterminacies such that source signals can only be identified up to a fixed permutation and some complex factors.

So far, the BSS problem has been solved using statiscal information available on the source signals. The first solution was based on the cancellation of higher order moments assuming non-Gaussian and iandependaent and identically distributed (IID) signals. Other solutions proposed the minimzation of cost functions such as contrast or likelihood functions. In the case of non-IID or even Gaussian sousces, second-order statistics were introduce to solve the problem.

When the frequency content of the source signals is time-varying, one can exploit the powerful tool of time-frequency distributions (TFD) to separate and recover the incomings signals. In contrast to conventional BSS approaches, the TFD-based techniques allow separation of correlated Gaussian sources with identical spectral shapes,

provided that the sources have different time-frequency signatures.

In this report, we start by laying the fundamentals of blind source separation along with some of the exisisting contrast functions inhereted from statistics. Then we briefly review the time-frequency representation basics before tackling the TFD-based contrasts, which lie at the heart of our work. We finish by a presentation of the algorithms and some numerical simulations to check their satisfactory results.

Contents

List of Notations

m	number of sources
n	number of sensors ($> m$)
$\mathbf{x}(t)$	received array signals
$\mathbf{s}(t)$	source signals (unknown)
$\mathbf{w}(t)$	zero-mean additive noise
$\mathbf{z}(t)$	an estimate of the source signals
$\mathbf{A}$	mixture matrix (unknown)
$\mathbf{B}$	separation matrix
$\mathbf{\Lambda}$	non-singular scale factor diagonal matrix
$\mathbf{P}$	permutation matrix
$G(\mathbf{z})$	contrast function
$\mathbf{s}^*$	(conjugate) transpose of the (complex) vector $\mathbf{s}$
$D_{ss}(t,f)$	Time-frequency distribution (TFD) of signal s
$D_{s_i s_j}(t,f)$	cross-TFD of two signals $s_i(t)$ and $s_j(t)$
$\mathrm{bfA}^{\#}$	pseudo-inverse of the matrix $\mathbf{A}$
$\mathcal{I}_{ij}$	interference-to-signal ratio
$\mathcal{I}_{\mathrm{perf}}$	global rejection index

List of Figures

Chapter 1

Blind Source Separation

This opening chapter is launched with the mathematical statement of the problem of separating mixed sources. Since the problem is reformulated into an estimation problem, unavoidable are the objective optimization functions and we dedicate the rest of this part to describing the exisisting specially tailored contrast functions.

1.1 Problem Statement

Assume that m signals strike an array of $n > m$ sensors. The measured array output is a weighted superposition of the signals, corrupted by additive noise

$$\mathbf{x}(t) = \mathbf{A}\mathbf{s}(t) + \mathbf{w}(t) \tag{1.1}$$

where $\mathbf{s}(t) = [s_1(t), s_2(t), \ldots, s_m(t)]^{\mathrm{T}}$ is the $m \times 1$ complex source signal vector containing the complex envelope of the emitter signals, $\mathbf{w}(t) = [w_1(t), w_2(t), \ldots, w_n(t)]^{\mathrm{T}}$

is the $n \times 1$ complex noise vector and $\mathbf{A} = [\mathbf{a_1}, \mathbf{a}_2, \ldots, \mathbf{a}_m]$ is the $n \times m$ full column rank mixture matrix. The source signal vector $\mathbf{s}(t)$ is assumed to be a multivariate non-stationary complex stochastic process. The components, s_i, are assumed to have different signatures in the time-frequency domain. The additive noise $\mathbf{w}(t)$ is modelled as a stationary zero-mean complex random process. The purpose of blind source separation is to find a separating matrix B such that $\mathbf{z}(t) = \mathbf{B}\mathbf{x}(t)$ is an estimate of the source signals. Before proceeding, note that a complete identification of the separating matrix **B,** or equivalently the mixing matrix **A,** is impossible in a blind context because the exchange of a fixed scalar between the source signal and the corresponding column of **A** leaves the observations **x** unaffected. Also note that the indexing of the signals is not very important. It follows that the best that can be done is to determine **B** up to permutation of its columns and some scalar shifts. Put otherwise, **B** is a separating matrix if and only if

$$\mathbf{z}(t) = \mathrm{P}\ \mathbf{\Lambda}\ \mathrm{s}(t) \tag{1.2}$$

where **P** is a permutation matrix and $\mathbf{\Lambda}$ a non-singular diagonal matrix.

1.2 Contrast Functions

Since we are dealing with an estimation problem, we have to introduce the cost functions which are to be minimized. A class of cost functions which has been invented especially to solve the BSS problem are the contrast functions [4]. Any contrast function $G(\mathbf{z})$ has to verify the following requirements:

- be a real-valued function of **z,**
- not change if the z_i are permuted,
- be invariant to scale changes, and
- increase by linear combination, i.e. for any matrix **C** invertible, $G(\mathbf{Cz}) \geq G(\mathbf{z})$.

1.2.1 Second Order Statistics Contrasts

The source signal vector $\mathbf{s}(t)$ is assumed to be a multivariate zero-mean stationary complex stochastic process with second order moments:

$$\mathbf{S}(\tau) = E[\mathbf{s}(t+\tau)\mathbf{s}^*(t)] = \text{diag}[\rho_1(\tau), \ldots, \rho_n(\tau)] \tag{1.3}$$

where $\rho_i(\tau) = E[\mathbf{s}_i(t+\tau)\mathbf{s}_i^*(t)]$, $E[.]$ denoting mathematical expectation and $\mathbf{s}^*$ the (conjugate) transpose of the (complex) vector **s**. We present two separation criterion for the stationary, temporally correlated source signals [12]. Consider first the noiseless case.

Theorem 1.1 *Let $\tau_1, \ldots, \tau_K$ be $K \geq 1$ (non-zero) time lags and define the $1 \times (K+1)$ vector $\rho_i = [\rho_i(0), \rho_i(\tau_1), \ldots, \rho_i(\tau_K)]$, $0 < i \leq n$. Then BSS can be achieved using the output correlation matrices at time lags $0, \tau_1, \ldots, \tau_K$ if and only if:*

$$\rho_i \text{ and } \rho_j \text{ are linearly independent for } i \neq j \tag{1.4}$$

*Assume that(1.4) holds and let $\mathbf{z}(t)$ be an $n \times 1$ vector given by $\mathbf{z}(t) = \mathbf{Bx}(t)$. Define $r_{ij}(k) = E[\mathbf{z}_i(t+k)\mathbf{z}_j^*(t)]$. Then, **B** is a separating matrix if and only if*

$$r_{ij}(k) = 0 \text{ and } r_{ii}(0) > 0 \tag{1.5}$$

for all $1 \leq i \neq j \leq n$ *and* $k = 0, \tau_1, \ldots, \tau_K$.

For the noisy case we have:

Theorem 1.2 *Let* $\tau_1, \ldots, \tau_K$ *be* $K \geq 1$ *(non-zero) time lags and define the* $1 \times K$ *vector* $\rho_i = [\rho_i(\tau_1), \ldots, \rho_i(\tau_K)]$, $0 < i \leq n$. *Then BSS can be achieved using the output correlation matrices at time lags* $\tau_1, \ldots, \tau_K$ *if and only if:*

$$\rho_i \text{ and } \rho_j \text{ are linearly independent for } i \neq j \tag{1.6}$$

Assume that (1.6) holds and let $\mathbf{z}(t)$ *be an* $n \times 1$ *vector given by* $\mathbf{z}(t) = \mathbf{B}\mathbf{x}(t)$. *Define* $r_{ij}(k) = E[\mathbf{z}_i(t+k)\mathbf{z}_j^*(t)]$. *Then,* $\mathbf{B}$ *is a separating matrix if and only if*

$$r_{ij}(k) = 0 \text{ and } \sum_{k=\tau_0}^{\tau_K} |r_{ii}(k)| > 0 \tag{1.7}$$

for all $1 \leq i \neq j \leq n$ *and* $k = \tau_1, \ldots, \tau_K$.

We can see that in the trivial case where the sources show identical normalized spectra, conditions (1.4) and (1.6) cannot be satisfied and thus separation will not be achieved. Conversely, when the source signals have different normalized spectra, it is always possible (with certainty) to find a set of time lags $\tau_1, \ldots, \tau_K$ such that (1.4) and (1.6) are met. This corresponds to the second-order identifiability condition found in [13]. It is worth to point out that this condition is necessary and sufficient for BSS using the whole set of SOS statistics while condition (1.4) (resp. (1.6)) is a necessary and sufficient condition for BSS using a finite set of correlation coefficients including (resp. excluding) the zero-lag one.

In the noiseless case, to solve the separating conditions (1.5), we consider the following least squares error criterion:

$$G_1(\mathbf{z}) = \sum_{k=\tau_0}^{\tau_K} \sum_{1 \le i < j \le m} [|r_{ij}(k) + r_{ji}(k)|^2 + |r_{ij}(k) - r_{ji}(k)|^2] + \sum_{i=1}^{m} |r_{ii}(0) - 1|^2 \quad (1.8)$$

(with $\tau_0 = 0$). It is easy to see that $G_1(\mathbf{z})$ is a contrast function which minimization is equivalent to solving (1.5). The separation criterion becomes

$$\mathbf{B} \text{ is a separating matrix} \equiv G_1[\mathbf{z}(t)] = 0 \quad (1.9)$$

where $\mathbf{z}(t) = \mathbf{B}\mathbf{x}(t)$.

For the noisy situation, the contrast function is defined with a similar separation criterion

$$G_2(\mathbf{z}) = \sum_{k=\tau_0}^{\tau_K} \sum_{1 \le i < j \le m} [|r_{ij}(k) + r_{ji}(k)|^2 + |r_{ij}(k) - r_{ji}(k)|^2] + \sum_{i=1}^{m} |r_{ii}(k) - 1|^2 \quad (1.10)$$

1.2.2 Higher Order Statistics Contrasts

Denote $\mathbf{z} \to g(\mathbf{z})$ a vector to vector non-linear odd function of $\mathbf{z}$, where the i-th coordinate of $g(\mathbf{z})$ is $w_i f_i(|z_i|^2) z_i$ with f_i is an odd differentiable real function and $w_i, \quad 1 \le i \le n$ are weights iteratively updated to improve the quality of the recovery of the desired signal with respect to the interference signals. And define the following mapping $\mathbf{z} \to G(\mathbf{z})$ from vector to matrix [14]:

$$G(\mathbf{z}) = \mathbf{z}\mathbf{z}^* - \mathbf{I} + (g(\mathbf{z})\mathbf{z}^* - \mathbf{z}g(\mathbf{z})^*) \quad (1.11)$$

where $\mathbf{I}$ is the identity matrix. If $\mathbf{z}$ is a white random vector with IID components, then the mean value of $G(\mathbf{z})$ is the null matrix in the noiseless case:

$$\mathbf{B} \text{ is a separating matrix } \equiv G_3(\mathbf{z}) = E[G(\mathbf{z})] = 0 \tag{1.12}$$

It is easy to note that $G_3(\mathbf{z})$ is also a contrast function which minimization leads to statistically independent estimates.

Chapter 2

Time-Frequency Concepts

In this chapter we review briefly the basics of time-frequency signal analysis. As need is mother of invention, we present the reasons that pushed analysts who dealt with non-conformist signals to resort to this new tool. Afterwards the most common time-frequency distributions are introduced with a special interest given to the ones that we will use in our experiments.

2.1 Need for a new tool

The two classical representations of a signal s are the time-domain representation $s(t)$, and the frequency-domain representation $S(f)$, and they form a Fourier Transform pair. Each representation in one variable is non localised with respect to the other variable and, therefore, is not suitable for signals with time-varying spectral contents (nonstationary signals), as widely found in real life applications, where an indication

is needed as to how the frequency content is changing with time [8].

To overcome these inadequacies, a representation in the two dimensional (t, f) space is much desired. Such a representation is intended to provide a distribution of signal energy versus time and frequency simultaneously and is called a time-frequency distribution (TFD). Another significant reason for the use of a time-frequency representation is that it reveals whether the signal is monocomponent or multicomponent, a fact that cannot be revealed by the two conventional representation specially when individual components are also time varying. Using the TFD, the start and stop time instants of the individual components are clearly identifiable.

2.2 Linear FM signals

We recall now some important definitions [10]. Let $s(t)$ be a real FM signal of the general form:

$$s(t) = A(t)cos[\theta(t)] \tag{2.1}$$

with the assumption that the spectra of the amplitude $A(t)$ and phase $\theta(t)$ are separated (nonoverlapping) in frequency, i.e. the signal approaches a narrowband condition.

Let $\mathcal{H}[.]$ denote the Hilbert Transform of the signal, such that

$$\mathcal{H}[s(t)] = s(t) \star \frac{1}{\pi t}$$

$$\mathcal{H}[s(t)] = \frac{1}{\pi}\mathcal{P}\left\{\int_{-\infty}^{\infty} \frac{s(\tau)}{t-\tau} d\tau\right\}$$

where $\mathcal{P}\{.\}$ is the Cauchy principle value of the improper integral given in this case by

$$\lim_{\delta \to 0} \left[\int_{-\infty}^{t-\delta} \frac{s(\tau)}{t-\tau} d\tau + \int_{t+\delta}^{\infty} \frac{s(\tau)}{t-\tau} d\tau \right] \tag{2.2}$$

A signal $z(t)$ defined as

$$z(t) \triangleq s(t) + j\mathcal{H}[s(t)] \approx A(t)e^{j\theta(t)} \tag{2.3}$$

is called the *analytic signal* of the real signal $s(t)$. The approximation is valid for the above narrowband condition. The definition of the analytic signal is necessary to introduce important characteristic of a signal $s(t)$.

Let $z(t)$ be an analytic signal given in the form

$$z(t) = A_z(t)e^{j\theta_z(t)} \tag{2.4}$$

The *instantaneous frequency* of signal z(t) is then defined as

$$f_i(t) \triangleq \frac{1}{2\pi} \frac{d\theta_z(t)}{dt} \tag{2.5}$$

The IF of a signal indicates the dominant frequency of the signal at a given time. In this sense, a signal is said to be nonstationary if its IF varies with time. Note that this definition applicable to monocomponent signals only, such as the signal illustrated in Fig. 2.1. When more than one "ridge" appears in the signal TF representation, the signal is said to be multicomponent, e.g. the signal in Fig. 2.2.

The nonstationarity can also be expressed in probabilistic terms. Let $z(t)$ be a complex signal of which the autocorrelation function is defined as :

$$\mathcal{R}(t,\tau) \triangleq E\left[z(t+\frac{\tau}{2}) z^*(t-\frac{\tau}{2}) \right] \tag{2.6}$$

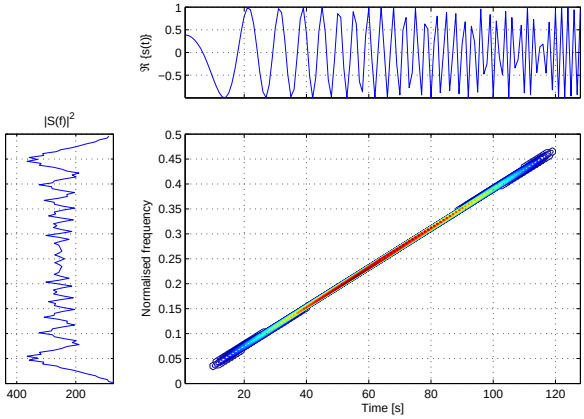

Figure 2.1: TF representation of an LFM signal

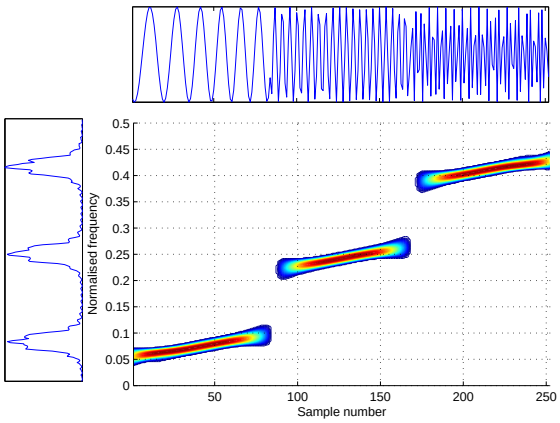

Figure 2.2: TF representation of a three-componentsignal

Note the use of symmetric points $t_1 = t + \tau/2$ and $t_2 = t - \tau/2$ in the previous definition. If $\mathcal{R}(t, \tau)$ only depends on the lag τ, which is the difference between t_1 and t_2, the signal $s(t)$ is said to be wide-sense stationary (WSS) where we have considered only the second-order moment. On the other hand, when this condition is not satisfied, $s(t)$ is said to be nonstationary and the autocorrelation function $\mathcal{R}(t, \tau)$ depends on both the time t and the lag τ.

Consider a typical FM transmission used in communication systems where a narrow-band FM signal is commonly defined as:

$$s(t) \triangleq A(t) \cos \left[2\pi f_c t + 2\pi \int_{-\infty}^{t} m(\tau) d\tau \right] \tag{2.7}$$

When $m(t)$ is a linear function of t, i.e. $m(t) = \alpha t$, the signal $s(t)$ is called a linearly frequency-modulated (LFM) signal. In addition, if $A(t)$ is a rectangular function the signal is called a *chirp.* A chirp signal, with duration T and bandwidth B, can be expressed as:

$$s^{\text{chirp}}(t) = \text{rect}_T(t) \cos \left[2\pi \left(f_c t + \frac{\alpha}{2} t^2 \right) \right]$$

where

$$\text{rect}_T(t) = \begin{cases} 1 & \text{for } 0 \leq t \leq T \\ 0 & \text{elsewhere} \end{cases}$$

The analytic signal associated with $s^{\text{chirp}}(t)$ is then given by

$$z^{\text{LFM}}(t) = \text{rect}_T(t) e^{j\theta(t)} = \text{rect}_T(t)\ e^{j2\pi(f_c t + \frac{\alpha}{2} t^2)} \tag{2.8}$$

and its IF is

$$f_i^{\text{chirp}}(t) = \frac{1}{2\pi} \frac{d\theta(t)}{dt} = f_c + \alpha t \tag{2.9}$$

Found in many applications, the chirp signal defined in 2.8 is the basic signal used in radar transmission, and can be easily generated. It is also used in military communication systems where the chirp is sent out as a hostile signal to destroy enemy transmissions. In this thesis, we will refer to the chirp signal as an LFM signal (i.e. the rectangular amplitude is implicit).

Based on the above definitions of analytic signals and instantaneous frequency for nonstationary signals, we are now ready and eager to see how they evolve in a time-frequency setting.

2.3 Time-Frequency Distributions

To study the spectral properties of a signal s at time t, an intuitive approach is to, first, take a slice of the signal by applying a moving window centered at time t and then calculate the spectrum magnitude of the windowed signal. Consider a signal $s(\tau)$ and a real even window $h(\tau)$, whose Fourier transform (FT) are $S(f)$ and $H(f)$, respectively. To obtain a localized spectrum of $s(\tau)$ at time $\tau = t$, multiply the signal by the window $h(\tau)$ centred at time $\tau = t$ and then take the FT with respect to τ, obtaining

$$S_h(t, f) = \mathcal{FT}_{\tau \to f}\{s(\tau)h(\tau - t)\} \tag{2.10}$$

$S_h(t, f)$ is called the short-time Fourier transform (STFT). The squared magnitude of the STFT, denoted by $\rho^{\text{SPEC}}(t, f)$ is called the spectrogram (SPEC). It can be

mathematically expressed as

$$\rho^{\mathrm{SPEC}}(t,f) = |S(t,f)|^2 = \left| \int_{-\infty}^{+\infty} s(\tau) h(\tau - t) e^{-j2\pi f\tau} d\tau \right|^2 \tag{2.11}$$

Another good example is the Wigner-Ville distribution which was derived as the Fourier transform of the symmetric autocorrelation of an analytical signal $z(t)$. Its time-frequency distribution (TFD) is

$$W_z(t,f) = \int_{-\infty}^{+\infty} z(t+\tau/2) z^*(t-\tau/2) e^{-j2\pi f\tau} d\tau \tag{2.12}$$

A knowledge of the time-lag signal kernel from $\tau = -\infty$ to $\tau = +\infty$, raises some problems in practice. That is why we introduce a regular window $h(\tau)$, leading to a new TFD called the pseudo Wigner-Ville distribution (PWVD):

$$PW_z(t,f) = \int_{-\infty}^{+\infty} h(\tau) z(t+\tau/2) z^*(t-\tau/2) e^{-j2\pi f\tau} d\tau \tag{2.13}$$

2.4 Cohen's Class

In a TFD, covariance in both variables is a very important property. This is commonly known as shift-covariance and it guarantees that when the signal is delayed in time and modulated frequency, the TFD is translated by the same quantities in the time-frequency plane. It has been shown that the class of energy time-frequency distributions verifying these foregoing properties possesses the following general expression:

$$\rho_z(t,f) = \int\int\int_{-\infty}^{+\infty} e^{j2\pi\nu(t-u)} g(\nu,\tau) z(u+\tau/2) z^*(u-\tau/2) e^{-j2\pi f\tau} d\nu du d\tau \tag{2.14}$$

where $g(\nu,\tau)$ is a two-dimensional function in the Doppler-lag domain (ν,τ), and is called the TFD Doppler-lag filter kernel. This class of distributions is known as the *Cohen's class*. The filter kernel determines the TFD and its properties. We can obtain a TFD with certain desired properties by properly constraining the $g(\nu,\tau)$ function. Eq. (2.14) can be simplified as

$$\rho_z(t,f) = W_z(t,f) \star_t \star_f \gamma(t,f) \tag{2.15}$$

The notation $\star_t\star_f$ in (2.15) represents a convolution in both t and f directions, and $\gamma(t,f)$ is the time-frequency kernel obtained through two-dimensional $\mathcal{FT}$ of $g(\nu,\tau)$: one $\mathcal{FT}$ operation from τ to $f$and one $\mathcal{FT}^{-1}$ operation from ν to t as:

$$\gamma(t,f) = \int\int_{-\infty}^{+\infty} g(\nu,\tau) e^{-j2\pi f\tau} e^{+j2\pi t\nu} d\tau d\nu \tag{2.16}$$

This is the definition (2.15) of the quadratic class of TFDs in terms of the WVD and the time-frequency kernel. For this raison we regard the WVD as a basic or prototype quadratic TFD, and all other quadratic TFDs as filtered version thereof.

We can also be express (2.14) in the time-lag domain as:

$$\rho_z(t,f) = \int\int_{-\infty}^{+\infty} \phi(t-u,\tau) z(u+\tau/2) z^*(u-\tau/2) e^{-j2\pi f\tau} du d\tau \tag{2.17}$$

where $\phi(t,\tau) = \mathcal{FT}^{-1}_{t\leftarrow\nu}\{g(\nu,\tau)\}$ is the time-lag filter kernel. The problem of cross-terms introduced by WVD when applying it to a multicomponent signal can be dealt with by selecting a suitable kernel $g(\nu,\tau)$ which minimises the cross-terms effectively. The corresponding TFD to such filter kernels are known as Reduced Interference Distributions (RID). The RID may be applied in situations where there are simultaneously a number of signals of interest which need to be separated. Examples of

time-frequency RID that will be used in the experiments are the Choi-Williams distribution (CWD) and the Born-Jordan distribution (BJD). Table 2.1 summarizes the aforementioned TFDs and their corresponding Doppler-lag kernels.

Name	**Doppler-lag Kernel**: $g(\nu,\tau)$	**TFD**: $\rho_z(t,f)$
WVD	1	$\int_{-\infty}^{+\infty} z(t+\tau/2)z^*(t-\tau/2)e^{-j2\pi f\tau}d\tau$
SPEC	$\int_{-\infty}^{+\infty} h(u+\frac{\tau}{2})h^*(u-\frac{\tau}{2})e^{-j2\pi\nu u}du$	$\lvert\int_{-\infty}^{+\infty} h(\tau-t)z(\tau)e^{-j2\pi f\tau}d\tau\rvert^2$
CWD	$e^{-\nu^2\tau^2/\sigma}$	$\int\int \frac{\sqrt{\pi\sigma}}{\lvert\tau\rvert}e^{\frac{-\pi^2\sigma(t-u)^2}{\tau^2}}z(t+\tau/2)z^*(t-\tau/2)e^{-j2\pi f\tau}dud\tau$
BJD	$\frac{\sin(2\pi\alpha\nu\tau)}{2\pi\alpha\nu\tau}$	$\int_{-\infty}^{+\infty}\int_{t-\lvert\alpha\tau\rvert}^{t+\lvert\alpha\tau\rvert}\frac{1}{2\alpha\tau}z(t+\tau/2)z^*(t-\tau/2)e^{-j2\pi f\tau}dud\tau$

Table 2.1 : Some common TFD and their filter kernels

2.4.1 Discrete Form

The discrete-time form of the Cohen's class TFDs, for a signal $s(t)$, is given by [8]

$$D_{ss}(t,f)=\sum_{l=-\infty}^{\infty}\sum_{q=-\infty}^{\infty}\phi(q,l)s(t+q+l)s^*(t+q-l)e^{-j4\pi fl} \tag{2.18}$$

where t and f represent the time index and the frequency index, respectively. The kernel $\phi(q,l)$ characterizes the distribution and is a function of both the time and lag variables. The cross-TFD of two signals $s_i(t)$ and $s_j(t)$ is defined by

$$D_{s_is_j}(t,f)=\sum_{l=-\infty}^{\infty}\sum_{q=-\infty}^{\infty}\phi(q,l)\ s_i(t+q+l)\ s_j^*(t+q-l)\ e^{-j4\pi fl}. \tag{2.19}$$

Chapter 3

TFD-Based Contrast Functions

After our discussion statistics based (second order and higher order) contrast function in the first chapter, we will introduce the contrasts that are inspired form the time frequency domain for the two classes of sources: uncorrelated and, the more interesting one, correlated.

3.1 Uncorrelated Sources

We present here a separation criterion [15] in the case of uncorrelated non-stationary source signals. We have the following result:

Theorem 3.1 *Let* $(t_1, f_1), \cdots (t_K, f_K)$ *be* K *time frequency points corresponding to signal auto-terms (i.e. energy concentration) and define* $1 \times K$ *vectors*

$$\mathbf{d}_i = [D_{s_i s_i}(t_1, f_1), \cdots, D_{s_i s_i}(t_K, f_K)], \qquad i = 1, \ldots, m.$$

Then BSS can be achieved if and only if

$$\mathbf{d}_i \text{ and } \mathbf{d}_j \text{ are linearly independent for } i \neq j \tag{3.1}$$

Assume that (3.1) holds and let $\mathbf{z}(t)$ *be an* $m \times 1$ *vector given by* $\mathbf{z}(t) = \mathbf{B}\mathbf{x}(t)$. *Then* $\mathbf{B}$ *is a separating matrix if and only if*

$$D_{z_i z_j}(t_k, f_k) = 0 \tag{3.2}$$

for all $1 \leq i \neq j \leq m$ *and* $k = 1, \cdots, K$, *and*

$$E[z_i(t) z_j(t)^*] = \delta_{ij} \tag{3.3}$$

where δ_{ij} *denotes the Kronecker operator.*

Proof: Let us write $\mathbf{z}(t) = \mathbf{C}\mathbf{s}(t)$ where $\mathbf{C} = \mathbf{B}\mathbf{A}$. Equations (3.2) and (3.3) are equivalent to $\mathbf{C}$ unitary. Herein, thanks to the inherent indeterminacy of the blind source separation, we have assumed without any loss of generality that $E[\mathbf{s}(t)\mathbf{s}(t)^*] = \mathbf{I}$ where $\mathbf{I}$ is the identity matrix. Also we have $\mathbf{C}\mathbf{D}_{\mathbf{ss}}(t_k, f_k)\mathbf{C}^H$ diagonal for $k = 1, \ldots, K$. We can then conclude that $\mathbf{C} = \mathbf{P}\mathbf{\Lambda}$ where $\mathbf{P}$ is a permutation matrix and Λ a unitary diagonal matrix by using Theorem 2 of [6]. Let us now show that condition (3.1) is necessary to achieve blind source separation when using data time frequency distribution matrices $\mathbf{D}_{\mathbf{xx}}(t_k, f_k), k = 1, \ldots, K$. If two sources, say s_1 and s_2, have same time frequency signatures, i.e., $D_{s_1 s_1}(t_k, f_k) = D_{s_2 s_2}(t_k, f_k)$ for $k = 1, \ldots, K$, then any 'virtual' signal of the form $\tilde{\mathbf{x}}(t) = \tilde{\mathbf{A}}\tilde{\mathbf{s}}(t) + \mathbf{w}(t)$ where $\tilde{\mathbf{A}} = [\tilde{\mathbf{a}_1}, \tilde{\mathbf{a}_2}, \mathbf{a}_3, \ldots, \mathbf{a}_m]$ and

$\tilde{\mathbf{s}}(t) = [\tilde{s_1}(t), \tilde{s_2}(t), s_3(t), \ldots, s_m(t)]^T$ with

$$[\tilde{\mathbf{a}_1}, \tilde{\mathbf{a}_2}] = [\mathbf{a}_1, \mathbf{a}_2] \begin{bmatrix} \cos(\theta) & \sin(\theta) \\ -\sin(\theta) & \cos(\theta) \end{bmatrix} \tag{3.4}$$

and

$$\begin{bmatrix} \tilde{s_1} \\ \tilde{s_2} \end{bmatrix} = \begin{bmatrix} \cos(\theta) & -\sin(\theta) \\ \sin(\theta) & \cos(\theta) \end{bmatrix} \begin{bmatrix} \tilde{s_1} \\ \tilde{s_2} \end{bmatrix} \tag{3.5}$$

verifies $\mathbf{D}_{\tilde{\mathbf{x}}\tilde{\mathbf{x}}}(t_k, f_k) = \mathbf{D}_{\mathbf{xx}}(t_k, f_k)$ for $k = 1, \ldots, K$.

From Theorem 3.1 result, we can define a contrast function as follows:

$$G_4(\mathbf{z}) = \sum_{k=1}^{K} \sum_{1 \le i \ne j \le m} |D_{z_i z_j}(t_k, f_k)|^2 + |E[z_i z_j^*]|^2 + \sum_{i=1}^{m} |E[z_i z_i^*] - 1|^2 \tag{3.6}$$

and a separating matrix $\mathbf{B}$ can be computed by

$$\mathbf{B} = \text{Argmin}\,[G_4(\mathbf{Bx})]$$

From condition (3.3), it appears that the sources should be uncorrelated.

3.2 Correlated Sources

For non-stationary correlated source signals, we have the following result:

Theorem 3.2 *Let again $(t_1, f_1), \cdots (t_K, f_K)$ be K time frequency points corresponding to signal auto-terms and define $1 \times K$ vectors*

$$\mathbf{d}_i = [D_{s_i s_i}(t_1, f_1), \ldots, D_{s_i s_i}(t_K, f_K)], \qquad i = 1, \ldots, m.$$

Then Blind source separation can be achieved if and only if

$$\mathbf{d}_i \text{ and } \mathbf{d}_j \text{ are linearly independent for } i \ne j \tag{3.7}$$

Assume that (3.7) holds and let $\mathbf{z}(t)$ *be an* $m \times 1$ *vector given by* $\mathbf{z}(t) = \mathbf{B}\mathbf{x}(t)$. *Then* $\mathbf{B}$ *is a separating matrix if and only if*

$$D_{z_i z_j}(t_k, f_k) = 0 \tag{3.8}$$

for all $1 \leq i \neq j \leq m$ *and* $k = 1, \ldots, K$, *and*

$$\sum_{k=1}^{K} D_{z_i z_i}(t_k, f_k) = 1 \tag{3.9}$$

Proof: Let us write $\mathbf{z}(t) = \mathbf{C}\mathbf{s}(t)$ where $\mathbf{C} = \mathbf{B}\mathbf{A}$. Then, equations (3.8) and (3.9) are equivalent to

$$\mathbf{C}\mathbf{D}_{\mathbf{ss}}(t_k, f_k)\mathbf{C}^H \quad \text{diagonal for} \quad k = 1, \ldots, K$$

and

$$\mathbf{C}\left\{\sum_{k=1}^{K} \mathbf{D}_{\mathbf{ss}}(t_k, f_k)\right\}\mathbf{C}^H = \mathbf{I}$$

Note that $\sum_{k=1}^{K} \mathbf{D}_{\mathbf{ss}}(t_k, f_k)$ is a positive definite diagonal matrix as long as the time frequency points (t_k, f_k), $k = 1, \ldots, K$, correspond to signal auto-terms. Hence, the latter equation implies that $\mathbf{C}$ is unitary. Again, because of the inherent indeterminacy of the blind source separation, we assume without loss of generality that $\sum_{k=1}^{K} \mathbf{D}_{\mathbf{ss}}(t_k, f_k) = \mathbf{I}$. We can then conclude as for Theorem 3.1 that $\mathbf{C} = \mathbf{P}\mathbf{\Lambda}$ where $\mathbf{P}$ is a permutation matrix and $\mathbf{\Lambda}$ a unitary diagonal matrix by using Theorem 2 of [6]. The proof of the necessary condition of Theorem 3.1 holds also for Theorem 3.2.

From Theorem 3.2 result, we can define the following contrast function:

$$G_5(\mathbf{v}) = \sum_{k=1}^{K} \sum_{1 \leq i \neq j \leq m} |D_{z_i z_j}(t_k, f_k)|^2 + \sum_{i=1}^{m} |\sum_{k=1}^{K} D_{z_i z_i}(t_k, f_k) - 1|^2 \tag{3.10}$$

and a separating matrix $\mathbf{B}$ can be computed by

$$\mathbf{B} = \text{Argmin}\left[G_5(\mathbf{Bx})\right].$$

It appears clearly from the results of Theorem 3.2 that the usual assumption of uncorrelated sources in BSS is relaxed. Hence, in contrast to High Order Statistics (HOS) based separation techniques and Second Order Statistics (SOS) based methods, the new proposed blind separation technique based on the contrast function G_2 allows the separation of correlated Gaussian sources with identical spectral shape provided that the sources are non stationary with different time-frequency signatures.

Note that in the derivation of the contrast functions G_4 and G_5, the contribution of the additive noise has been neglected. However, the algorithms obtained from the new proposed contrast functions are expected to be robust with respect to noise because of the effects of spreading the noise power while localizing the source energy in the time-frequency domain. This amounts to increasing the local Signal-to-Noise Ratio (SNR).

Chapter 4

Algorithm Derivation

The theorems enonciated in the previous chapters (1 and 3) concerning the contrast functions are elegant but are not self sufficient. They need the introduction of some iterative techniques to satisfy the given separation criterion. Further in the chapter, we will exibit five algorithms, each corresponding to the afore mentioned theorems.

4.1 Iterative optimization algorithms

The separation criterion we have presented takes the form

$$\mathbf{B} \text{ is a separating matrix } \Rightarrow G(\mathbf{z}(t)) = 0 \tag{4.1}$$

where G is a given contrast function. The approach we chose to solving (4.1) is inspired by [11]. This approach is a block technique based on the processing of T received samples and consists of searching the zeros of the sample version of (4.1).

Solutions are obtained iteratively in the form

$$\mathbf{B}^{(p+1)} = (\mathbf{I} + \mathcal{E}^{(\mathbf{p})})\mathbf{B}^{(p)}$$

and thus

$$\mathbf{z}^{(p+1)}(t) = (\mathbf{I} + \mathcal{E}^{(\mathbf{p})})\mathbf{z}^{(p)}(t)$$

At step p, a matrix $\mathcal{E}^{(\mathbf{p})}$ is determined from a local linearization of $G[\mathbf{Bx}(t)]$. It is an approximate Newton technique with the benefit that $\mathcal{E}^{(\mathbf{p})}$ can be very simply computed (no Hessian inversion is needed) under the additional assumption that $\mathbf{B}^{(p)}$ is close to a separating matrix.

Moreover, one should bear in mind that the optimization of the TFD based contrast function requires the selection of a set of time frequency points corresponding to signal auto terms. An intuitive procedure to select these points is to consider the time frequency points corresponding to the maximum energy in the time frequency plane [6].

4.2 Algorithm SOS1

1. Initialization

$$\mathbf{z}(t) = \mathbf{x}(t), \quad t = 1, \ldots, T.$$

2. Update the correlation matrices $\mathbf{R}(k) = E[\mathbf{z}(t+k)\mathbf{z}^*(t)]$, $k = 0, \tau_1, \ldots, \tau_K$, using the following averaging technique:

$$\mathbf{R}^{(p)}(k) = \frac{1}{T-k} \sum_{t=1+k}^{T} \mathbf{z}(t)\mathbf{z}^*(t-k).$$

Note that $r_{ij}^{(p)}(k)$ is the (i,j)-th entry of $R^{(p)}(k)$ and that they form the vectors

$$\mathbf{r}_{ij}^{(p)} = \left[r_{ij}^{(p)}(0), r_{ij}^{(p)}(\tau_1), \ldots, r_{ij}^{(p)}(\tau_K)\right]^{\mathrm{T}}$$

3. Estimate $\epsilon_{ij}^{(p)}$

$$\begin{aligned}
\epsilon_{ii}^{(p)} &= \frac{1 - r_{ii}^{(p)}(0)}{2r_{ii}^{(p)}(0)} \\
\mathcal{E}_{ij}^{(p)} &= -([\mathbf{r}_{jj}^{(p)} \quad \mathbf{r}_{ii}^{(p)}]^{\#}[\frac{1}{2}(\mathbf{r}_{ij}^{(p)} + \mathbf{r}_{ji}^{(p)}) \quad \frac{1}{2j}(\mathbf{r}_{ij}^{(p)} - \mathbf{r}_{ji}^{(p)})]) \\
\mathcal{E}_{ij}^{(p)} &= \begin{bmatrix} \mathrm{Re}(\epsilon_{ij}^{(p)}) & \mathrm{Re}(\epsilon_{ji}^{(p)}) \\ \mathrm{Im}(\epsilon_{ij}^{(p)}) & -\mathrm{Im}(\epsilon_{ji}^{(p)}) \end{bmatrix}.
\end{aligned}$$

4. Update the value of the separating matrix and the correlation matrices for $k = 0, \tau_1, \ldots, \tau_K$:

$$\mathbf{B}^{(p+1)} = (\mathbf{I} + \mathcal{E}^{(p)})\mathbf{B}^{(p)}.$$

5. Update the estimated sources $\mathbf{z}(t)$:

$$\mathbf{z}^{(p+1)}(t) = (\mathbf{I} + \mathcal{E}^{(p)})\mathbf{z}^{(p)}(t) \quad \text{for} \quad t = 1, \ldots, T.$$

6. Stop or go to step 2

4.3 Algorithm SOS2

1. Initialization

$$\mathbf{z}(t) = \mathbf{x}(t), \quad t = 1, \ldots, T.$$

2. Update the correlation matrices $\mathbf{R}(k) = E[\mathbf{z}(t+k)\mathbf{z}^*(t)]$, $k = 0, \tau_1, \ldots, \tau_K$, using the following averaging technique:

$$\mathbf{R}^{(p)}(k) = \frac{1}{T-k} \sum_{t=1+k}^{T} \mathbf{z}(t)\mathbf{z}^*(t-k).$$

Note that $r_{ij}^{(p)}(k)$ is the (i,j)-th entry of $R^{(p)}(k)$ and that they form the vectors

$$\mathbf{r}_{ij}^{(p)} = \left[r_{ij}^{(p)}(0), r_{ij}^{(p)}(\tau_1), \ldots, r_{ij}^{(p)}(\tau_K)\right]^{\mathrm{T}}$$

3. Estimate $\epsilon_{ij}^{(p)}$

$$\begin{aligned}
\epsilon_{ii}^{(p)} &= \frac{1 - \sum_{k=\tau_1}^{\tau_K} |r_{ii}^{(p)}(k)|}{2\sum_{k=\tau_1}^{\tau_K} |r_{ii}^{(p)}(k)|} \\
\mathcal{E}_{ij}^{(p)} &= -([\tilde{\mathbf{r}}_{jj}^{(p)} \quad \tilde{\mathbf{r}}_{ii}^{(p)}]^{\#}[\frac{1}{2}(\tilde{\mathbf{r}}_{ij}^{(p)} + \tilde{\mathbf{r}}_{ji}^{(p)}) \quad \frac{1}{2j}(\tilde{\mathbf{r}}_{ij}^{(p)} - \tilde{\mathbf{r}}_{ji}^{(p)})]) \\
\mathcal{E}_{ij}^{(p)} &= \begin{bmatrix} \mathrm{Re}(\epsilon_{ij}^{(p)}) & \mathrm{Re}(\epsilon_{ji}^{(p)}) \\ \mathrm{Im}(\epsilon_{ij}^{(p)}) & -\mathrm{Im}(\epsilon_{ji}^{(p)}) \end{bmatrix}
\end{aligned}$$

4. Update the value of the separating matrix and the correlation matrices for $k = 0, \tau_1, \ldots, \tau_K$:

$$\mathbf{B}^{(p+1)} = (\mathbf{I} + \mathcal{E}^{(p)})\mathbf{B}^{(p)}.$$

5. Update the estimated sources $\mathbf{z}(t)$:

$$\mathbf{z}^{(p+1)}(t) = (\mathbf{I} + \mathcal{E}^{(p)})\mathbf{z}^{(p)}(t) \quad \text{for} \quad t = 1, \ldots, T.$$

6. Stop or go to step 2

4.4 Algorithm HOS

1. Initialization

$$\mathbf{z}(t) = \mathbf{x}(t), \quad t = 1, \ldots, T.$$

2. Evaluate the entries of matrix $\mathcal{E} = [\epsilon_{ij}]$, $1 \leq i, j \leq n$ as follows:

$$\epsilon_{ij} = \frac{\rho_{ii}\beta_{ij} + \alpha^*_{ji}(\delta_{ij} - \rho_{ij})}{\rho_{ii}\alpha_{ij} + \alpha^*_{ji}\rho_{jj}}$$

with

$$\begin{aligned}
\rho_{ij} &= \frac{1}{T}\sum_{t=1}^{T} z_i(t)z_j^*(t) \\
\alpha_{ij} &= \frac{1}{T}\sum_{t=1}^{T} |z_j(t)|^2\{f_i'(|z_i(t)|^2)|z_j(t)|^2 + f_i(|z_i(t)|^2) - f_j(|z_j(t)|^2)\} \\
\beta_{ij} &= \frac{1}{T}\sum_{t=1}^{T} z_i(t)z_j^*(t)\{f_j(|z_j(t)|^2)|z_j(t)|^2 - f_i(|z_i(t)|^2)\}
\end{aligned}$$

where f_i is a real function.

3. Update the source estimates:

$$\mathbf{z}(t) \leftarrow (\mathbf{I} + \mathcal{E})\mathbf{z}(t), \text{ for } t = 1, \ldots, T.$$

4. Stop or go to step 2

4.5 Algorithm TFD1

1. Initialization

$$\mathbf{z}(t) = \mathbf{x}(t), \quad t = 1, \ldots, T.$$

2. Evaluate the entries of matrix ϵ as follows:

$$\begin{aligned}
\rho_{ij} &= \frac{1}{T}\sum_{t=1}^{T} z_i(t)z_j^*(t) \\
\epsilon_{ii} &= \frac{1-\sigma_{ii}}{2\sigma_{ii}} \\
\mathcal{E}_{ij} &= -\mathrm{Re}([\tilde{\mathbf{d}_{jj}} \;\; \tilde{\mathbf{d}_{ii}}]^{\#}[\mathrm{Re}(\tilde{\mathbf{d}_{ij}}) \;\; \mathrm{Im}(\tilde{\mathbf{d}_{ij}})]) \\
\mathcal{E}_{ij} &= \begin{bmatrix} \mathrm{Re}(\epsilon_{ij}) & \mathrm{Re}(\epsilon_{ji}) \\ \mathrm{Im}(\epsilon_{ij}) & -\mathrm{Im}(\epsilon_{ji}) \end{bmatrix} \\
d_{ij}(t,f) &= \sum_{l,q=-T}^{T} \phi(q,l)z_i(t+q+l)\; z_j^*(t+q-l)e^{-j4\pi fl} \\
\tilde{\mathbf{d}_{ij}} &= [\sigma_{ij}, d_{ij}(t_1,f_1),\ldots,d_{ij}(t_K,f_K)]^{\mathrm{T}}
\end{aligned}$$

3. Update the source estimates:

$$\mathbf{z}(t) \leftarrow (\mathbf{I}+\mathcal{E})\mathbf{z}(t), \text{ for } \; t=1,\ldots,T.$$

4. Stop or go to step 2

4.6 Algorithm TFD2

1. Initialization

$$\mathbf{z}(t) = \mathbf{x}(t), \quad t=1,\ldots,T.$$

2. Evaluate the entries of matrix ϵ as follows:

$$\begin{aligned}
\gamma_{ii} &= \sum_{k=1}^{K} d_{ii}(t_k, f_k) \\
\epsilon_{ii} &= \frac{1-\gamma_{ii}}{2\gamma_{ii}} \\
\mathcal{E}_{ij} &= -\mathrm{Re}([\mathbf{d}_{jj} \;\; \mathbf{d}_{ii}]^{\#}[\mathrm{Re}(\mathbf{d}_{ij}) \;\; \mathrm{Im}(\mathbf{d}_{ij})]) \\
\mathcal{E}_{ij} &= \begin{bmatrix} \mathrm{Re}(\epsilon_{ij}) & \mathrm{Re}(\epsilon_{ji}) \\ \mathrm{Im}(\epsilon_{ij}) & -\mathrm{Im}(\epsilon_{ji}) \end{bmatrix} \\
\mathbf{d}_{ij} &= [d_{ij}(t_1, f_1), \ldots, d_{ij}(t_K, f_K)]^{\mathrm{T}} \\
d_{ij}(t,f) &= \sum_{l,q=-T}^{T} \phi(q,l) z_i(t+q+l) \; z_j^*(t+q-l) e^{-j4\pi f l}
\end{aligned}$$

3. Update the source estimates:

$$\mathbf{z}(t) \leftarrow (\mathbf{I} + \mathcal{E})\mathbf{z}(t), \text{ for } \; t = 1, \ldots, T.$$

4. Stop or go to step 2

Chapter 5

Numerical Simulation

The closing chapter contains all the experiments we have conducted to prove our practical achievements. We start off with the description of the performance index that will help us measure the impact of our new method with numbers and not just through the many plots we have generated. The two samples we have used to test our algorithms are presented, namely the linearly frequency modulated and the frequency-hopping modulated signals. Then we dip the input signals into noise and conduct our experiments. The results are very promising.

5.1 Performance index

Rather than estimating the variance of the coefficients of the mixing matrix, it is more relevant with respect to the source separation issue to compute an index which quantifies the performance in terms of interference rejection, as follows [6]. Assume

that, at each time instant t, an estimate of the vector of source signals is computed by applying the pseudo-inverse of the estimated mixture matrix to the received signal $\mathbf{x}(t)$, i.e.

$$\mathbf{z}(t) = \mathbf{B}\mathbf{x}(t) = \mathbf{B}\mathbf{A}\mathbf{s}(t) + \mathbf{B}\mathbf{w}(t) \tag{5.1}$$

In general, we stress that this procedure is not optimal for recovering the source signals based on an estimate $\mathbf{B}$. For large enough sample size T, matrix $\mathbf{B}$ should be close to the true mixing matrix $\mathbf{A}$ so that $\mathbf{BA}$ is close to the identity matrix. The performance index used in the sequel is the interference-to-signal ratio (ISR), defined as:

$$\mathcal{I}_{ij} = E|(\mathbf{BA})_{ij}|^2. \tag{5.2}$$

This actually defines an ISR due to the fact that by our normalization convention ([2]) we have $\mathcal{I}_{ij} \simeq 1$ for large enough T. Thus $\mathcal{I}_{ij}$ measures the ratio of the power of the interference of the j-th source to the power of the ip-th source signal estimated as in (5.2). As a measure of the global quality of the separation, we also define a global rejection level:

$$\mathcal{I}_{\text{perf}} = \sum_{i \neq j} \mathcal{I}_{ij}. \tag{5.3}$$

5.2 Experiments and results

In our experiments, a 2-element uniform linear array, having a half wavelength sensor spacing, receives two signals in the presence of a stationary complex white noise. In all the experiments, the source signals arrive from different directions $\phi_1 = 0^\circ$ and

$\phi_2 = 20°$. The snapshot size is $T = 1024$ samples.

5.2.1 Sample runs

5.2.1.1 Two LFM's run

In this example, the sources are two linearly frequency-modulated (LFM) signals (chirps) as shown in Figure 5.1. The observed mixed sources are shown in figure 5.2 for a signal to noise ratio (SNR) of 30 dB.

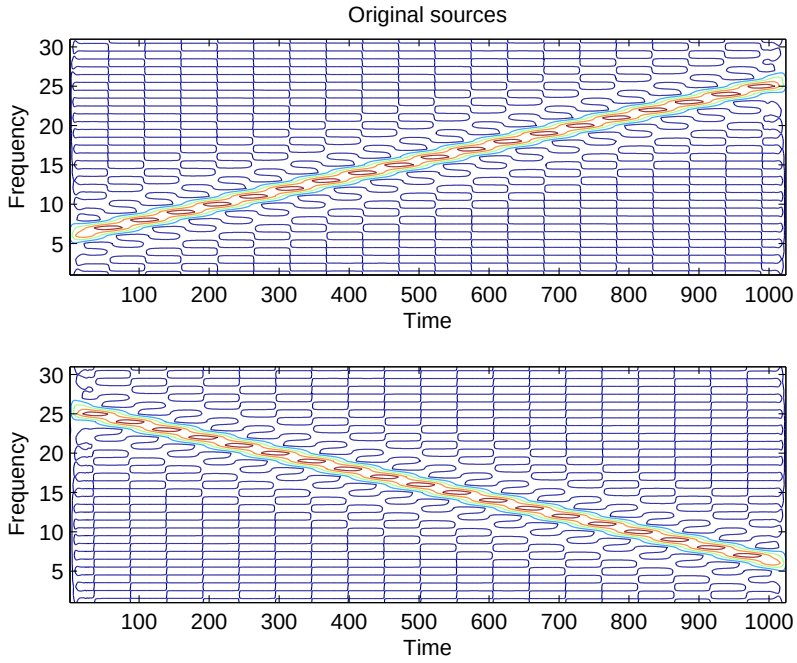

Figure 5.1: Original sources

Figures 5.3 and 5.4 show a sample run versus iterations of the algorithms TFD1 and TFD2, respectively. The TFD of each estimated source is plotted for each iteration. The signal to noise ratio (SNR) is set to 30 dB and the Choi-Williams distribution

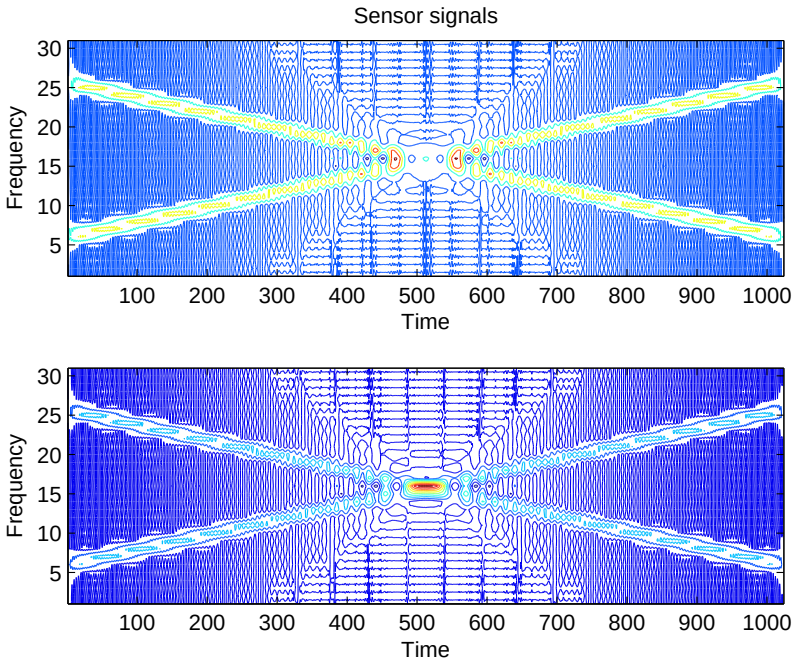

Figure 5.2: Sensor Signal SNR=30 dB

was selected for this example. It is clear from these two figures that the implemented algorithms converge in few iterations. Algorithm TFD1 seems to converge faster. This can be explained by the fact that in contrast to Algorithm TFD2, TFD2 requires the estimation of the covariance matrix, needing a few more iterations to achieve a sufficient accuracy.

5.2.1.2 Different input signals

In this example, the sources are one linear frequency modulated signal and a frequency hopping modulated signal as shown in Figure 5.5. The observed mixed sources are shown in Figure 5.6 for a signal to noise ratio (SNR)of 20 dB. Figures 5.7 and 5.8 show the estimated sources when using Algorithms TFD1 and TFD2, respectively.

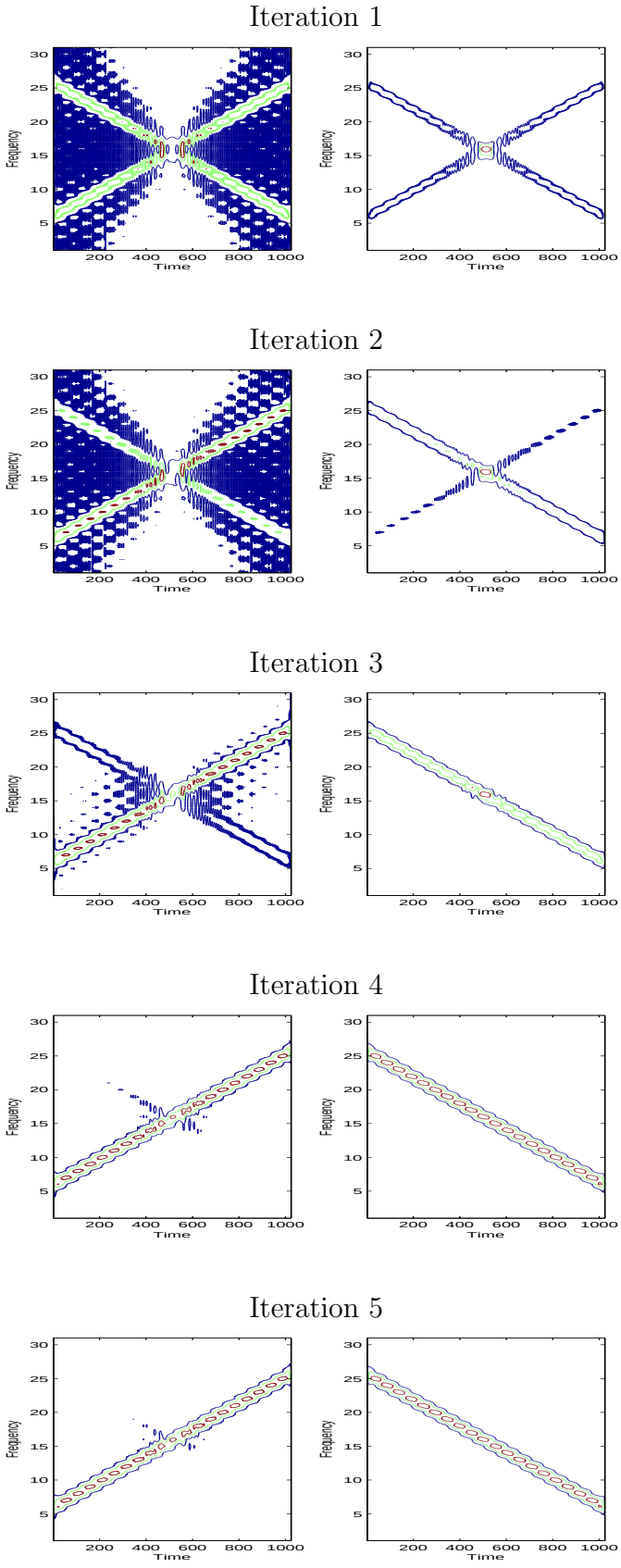

Figure 5.3: Sample run vs iterations: ALgorithm TFD1

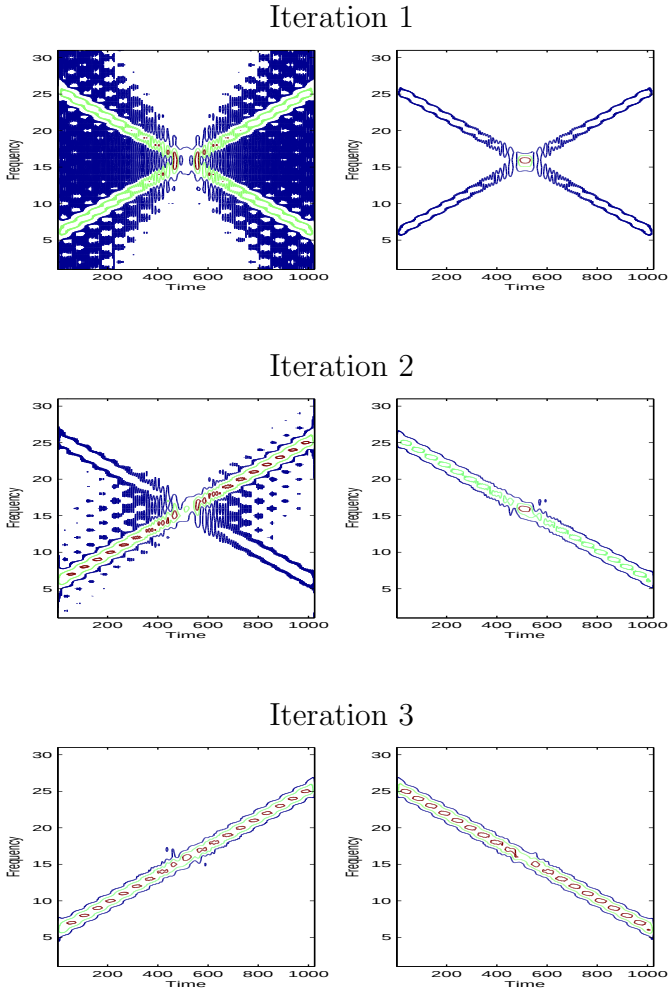

Figure 5.4: Sample run vs iterations: Algorithm TFD2

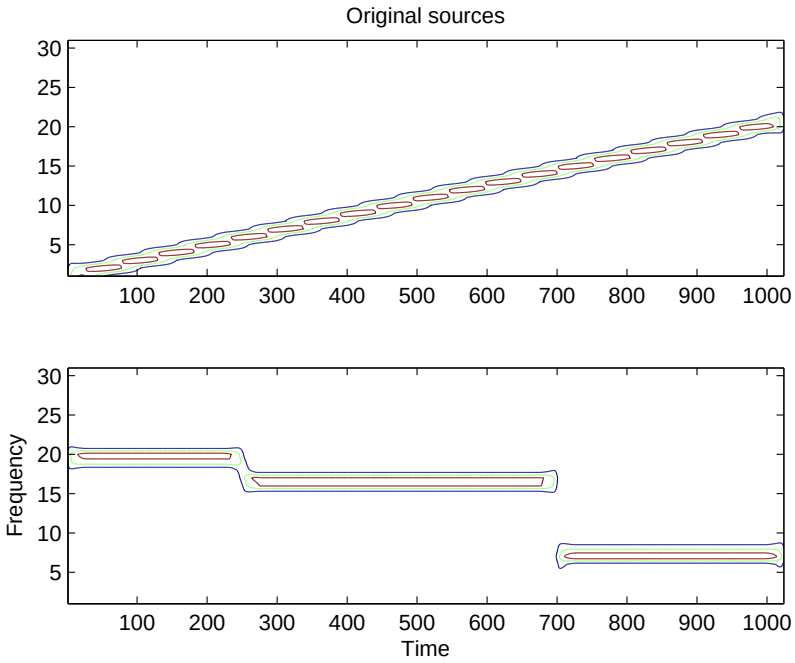

Figure 5.5: Original sources

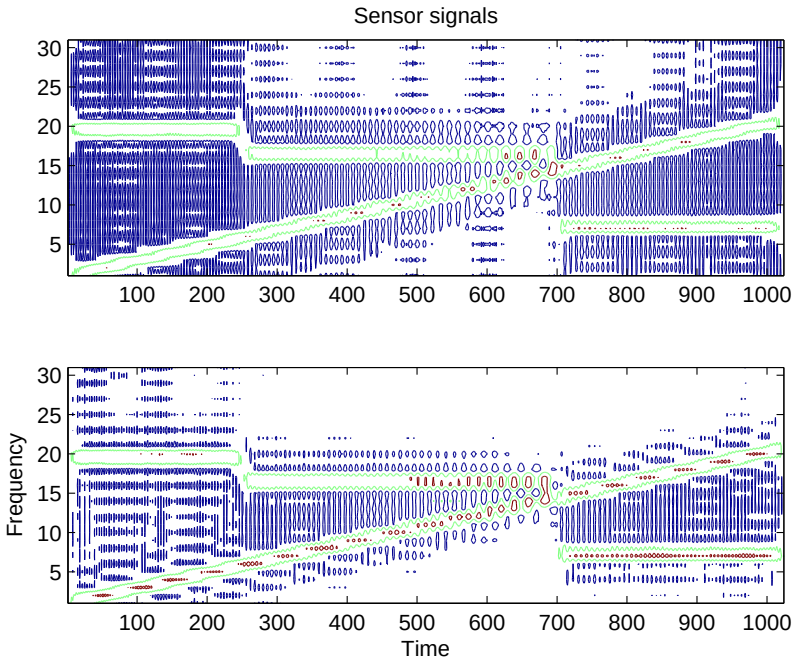

Figure 5.6: Sensor Signal SNR=20 dB

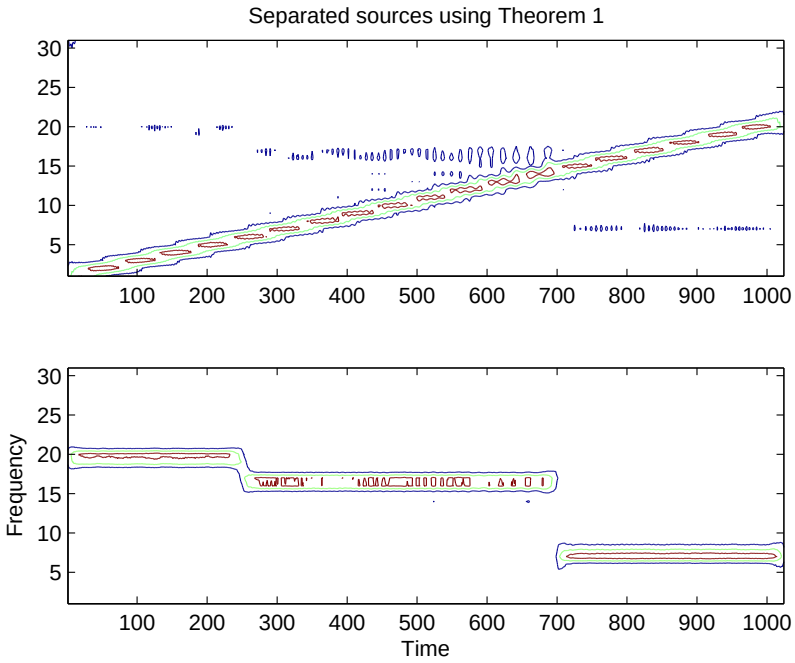

Figure 5.7: Separated sources using Algorithm TFD1

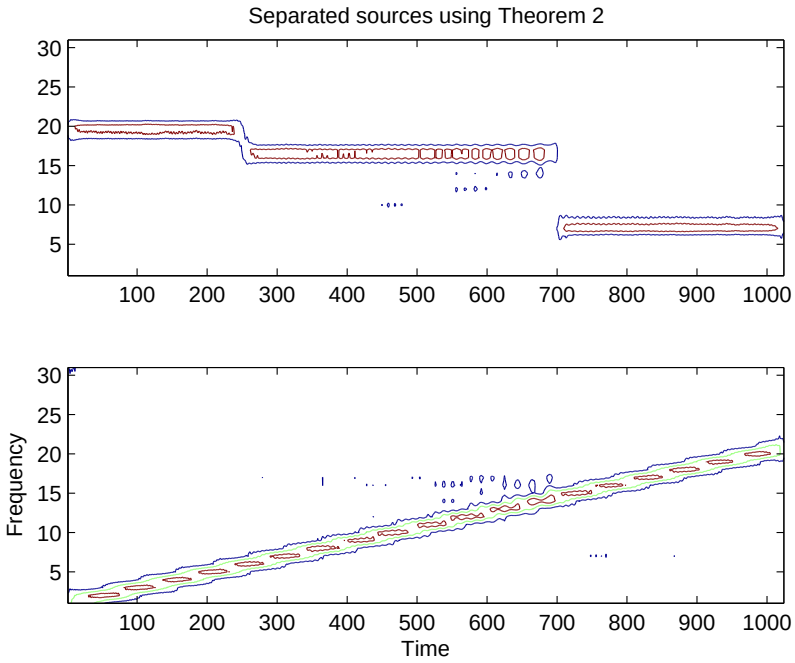

Figure 5.8: Separated sources using Algorithm TFD2

5.2.2 Noise Effect

Herein, we assess the performance of the TF based BSS algorithms with respect to the noise level. The chosen sources in this experiment are the two linear frequency modulated signals of Figure 5.1 .

In Figure 5.9, the rejection level $\mathcal{I}_{\text{perf}}$ is plotted in dB versus noise level (with respect to unity enegy input) for the five algorithms presented in this report: TFD1, TFD2, SOS1, SOS2, and HOS. The overall rejection level is obtained by averaging 100 independent trials and the Choi-Williams distribution was selected for this experiment. This figure shows clearly that the two TF based algorithms out perform the SOS and HOS based ones. In the case of our experiments, it can be explained as follows:

- the SOS-based BSS approach fails, since the sources have the same spectra shape, and
- the HOS-based BSS approach fails, since the sources have random Gaussian amplitudes.

5.2.3 TFD Kernel Effect

Herein, we assess the performance of the TF based BSS algorithms with respect to the TFD kernel. The chosen sources in this experiment are the two linear frequency modulated signals of Figure 5.1 .

Figures 5.10 and 5.11 give a comparison of the performance of the TF based contrast

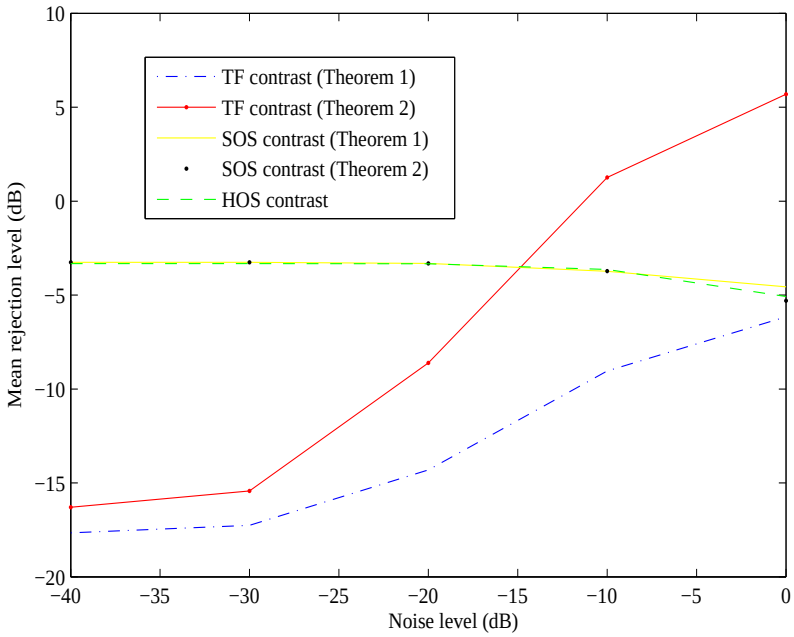

Figure 5.9: Performance comparison

function Algorithms 1 and 2, respectively, when choosing two different TFDs, namely, the Choi-Williams and Born-Jordan TFDs. According to these figures, the obtained results show better performance for low noise level when using the Born-Jordan TFD. This can be explained by the fact that the Born-Jordan TFD allows better estimation of the time-frequency auto term points than the Choi-Williams TFD.

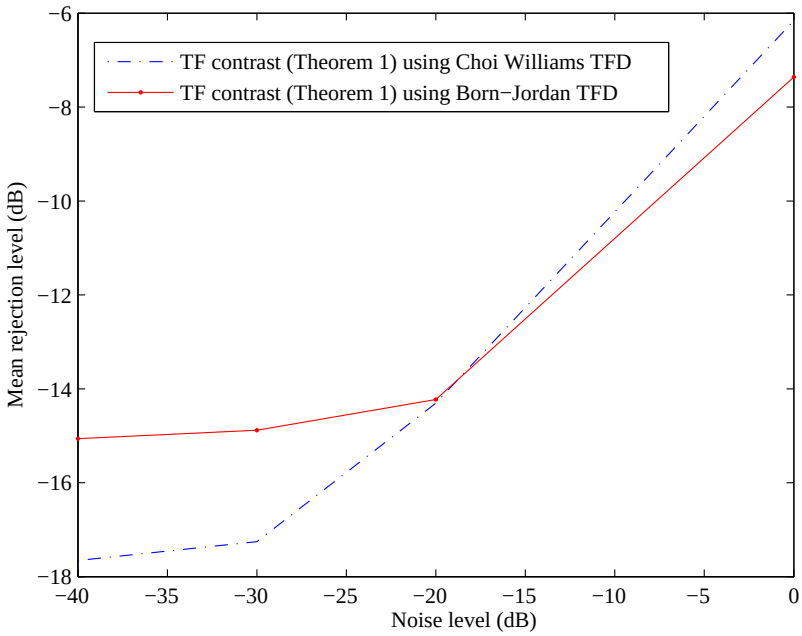

Figure 5.10: Performance comparison with respect to TFD1

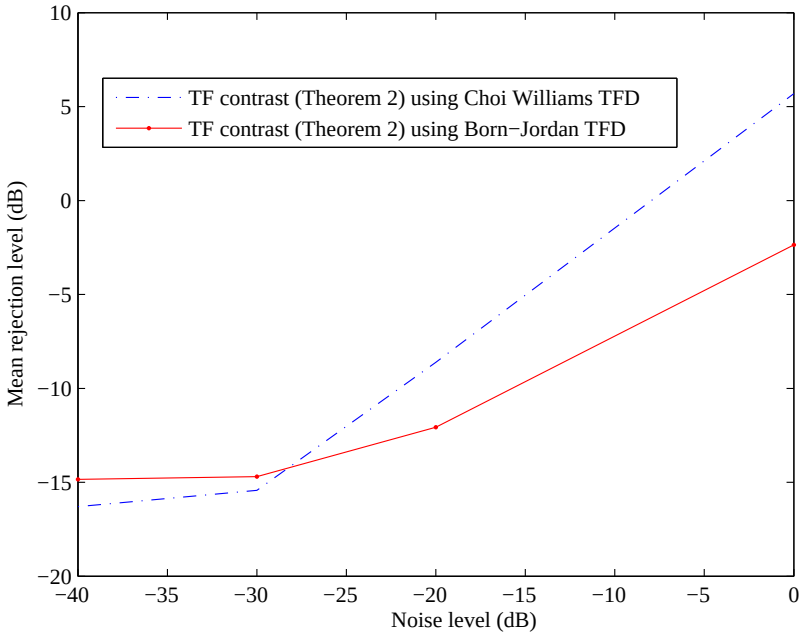

Figure 5.11: Performance comparison with respect to TFD2

CONCLUSION

This modest report presents the implementation and performance evaluation of two new blind source separation methods for non-stationary sources. Two TFD-based contrast functions are presented. Iterative algorithms, namely Algorithm TFD1 and TFD2, based on the relative gradient technique which minimizes the aforementioned contrast functions in order to perform the sought source separation are described. The performance of the TFD-based contrast functions are compared to the ones based on second order and higher order statistics. The obtained results show that the TFD-based techniques perform better, or to put it more precisely, are the only ones which separate non-stationary gaussian signals with identical spectral shape. We have used two basic signals that mimic real-life signals to test how the proposed methods react. In both cases, whether the frequency of the signal is changing smoothly (LFM) or abruptly (FHM), the results were statisfactory. Numerical experiments are carried out to evaluate the performance of the implemented TFD-based approach with respect to the selected time frequency distributions. It is shown that such a choice has an important impact on the targeted performance.

Now, what can the future have in store for this novel method? We can venture that the optimization method that has been used will not allow on-line processing, and

this is where adaptive optimization can be called for. Another venue could be to do a more rigorous mathematical performance analysis that would generate ideas on how to further improve the proposed algorithms.

Bibliography

[1] A. Belouchrani, K. Abed-Meraim, J.F. Cardoso, and E. Moulines, "Blind source separation using second order statistics," *IEEE Trans. on Sig. Proc.*, pp. 434–444, Feb. 1997.

[2] C. Jutten and J. Hérault, "Détection de grandeurs primitives dans un message composite par une architecture de calcul neuromimétrique en apprentissage non supervisé," in *Proc. Gretsi*, (Nice), 1985.

[3] P. Comon, "Independent component analysis, a new concept?," *Signal Processing*, vol. 36, pp. 287–314, 1994.

[4] J.-F. Cardoso, "Blind Signal Separation: Statistical Principles," *Proc. of the IEEE*, vol. 86, pp. 2009–2025, October 1998.

[5] A. Belouchrani and J.-F. Cardoso, "Maximum likelihood source separation for discrete sources," in *Proc. EUSIPCO*, pp. 768–771, 1994.

[6] A. Belouchrani and M. G. Amin, "Blind source separation based on time-frequency signal representation," *IEEE Trans. on Sig. Proc.*, pp. 2888–2898, Nov. 1998.

[7] J.F. Cardoso, A. Belouchrani, and B. Laheld, "new composite criterion for adaptive and iterative blind source separation", ICASSP'94, pp. 273–276.

[8] L. Cohen, *Time-frequency analysis*,Prentice Hall, 1995.

[9] P. Comon and C. Jutten, Editors, *Handbook of Blind Source Separation,* Academic Press, 2010.

[10] B. Boashash, Editor, *Time-Frequency Signal Analysis and Processing: A comprehensive reference,* Elsevier, Oxford, UK, 2003.

[11] D. T. Pham and P. Garat and C. Jutten, "Separation of a mixture of independent sources through a maximum likelihood approach," in Proc. EUSIPCO, pp. 771–774, 1992.

[12] Y. Xiang, K. Abed-Meriam, and Y. Hua, " Adaptive blind source separation by sescond order statistics and natural gradiant," in *Proc. ICASSP,* 1999.

[13] L. Tong, R. Liu, and Y. H. V. C. Soon, "Indeterminacy and Identifiability of Blind Identification," *IEEE Trans. on CS*, vol. 38, pp. 499–509, May 1991.

[14] A. Belouchrani and K. Abed-Meraim, "High Interference Rejection Rate Achieved Through an Adaptative Signal Separation," *Proc. ISSPA*, Brisbane, Australia, Aug. 1999.

[15] A. Belouchrani and K. Abed-Meraim, "Contrast Functions for Blind Source Separation Based on Time-Frequency Distributions," *Proc. ISCCSP*, Tunis, Tunisia, 2004.